

Optimization of Elman Neural Network Using Genetic Algorithm for Construction Cost Estimation and Overspending Risk Analysis

Qian Wu

School of Urban Construction, Anhui Xinhua University, Hefei 230088, Anhui, China

E-mail: wu2006qian@126.com

Keywords: neural network, construction cost estimation, overspending risk, Elman network, genetic algorithm

Received: November 14, 2024

This study proposes a model based on the Elman neural network and improves it using a Genetic Algorithm (GA) to increase the accuracy of construction cost estimation and accurately analyze the overspending risk. First, an index system containing multiple dimensions such as building features, structural features, project positioning, and project environment is constructed to comprehensively capture the key factors affecting construction cost and overspending risk. Second, the Elman neural network's structure and operation are thoroughly examined, and the GA optimizes the network's weights and thresholds to improve the model's predictive power. On the training set, the optimized GA-Elman model demonstrates great prediction accuracy, with relative error (RE) percentages between predicted and true values typically falling within $\pm 1\%$. On the test set, the GA-Elman model performs better than the original Elman model in both difference and RE, with a Mean Absolute Percentage Error of 2.75%, a decrease of 18.4% compared to the Elman model. These results indicate that the GA-Elman model is more accurate in cost prediction and more effective in identifying potential overspending risks. This study provides a powerful tool for cost control and budget management in the construction industry and a new perspective on the application of neural networks in construction economics.

Povzetek: Razvit je model za ocenjevanje stroškov gradnje in analizo tveganja prekoračitve stroškov, ki temelji na Elmanovi nevronske mreži, optimizirani z genetskim algoritmom. Model je močno orodje za obvladovanje stroškov in upravljanje proračuna v gradbeništvu.

1 Introduction

In the construction industry, cost estimation is the core link of project management, directly related to the project's economic benefits and risk control. Traditional cost estimation methods rely on expert experience and historical data. Still, such methods are often influenced by subjective judgment and are difficult to adapt to the rapidly changing market environment and complex and changing engineering conditions [1-3]. Traditional cost estimation procedures encounter increasing challenges as building projects get larger and more complicated. As a result, new techniques and methodologies must be introduced immediately to increase estimation efficiency and accuracy [4, 5].

With the advancement of machine learning (ML) and artificial intelligence in recent years, neural networks have shown to be a valuable tool for tackling challenging forecasting issues. Because of their benefits in processing sequence data, recurrent neural networks (RNNs) are widely applied across various fields, such as natural language processing and time series prediction [6-8]. The Elman neural network, as a kind of RNN, enhances the network's memory ability by introducing the context layer, which makes it perform well in dealing with time-dependent sequence data [9].

This study explores the application of neural networks in construction cost estimation and overspending risk analysis. A new approach to cost estimating is presented,

which involves creating a building cost model based on the Elman neural network and using a Genetic Algorithm (GA) to optimize it. This approach can increase cost estimating accuracy while evaluating potential overspending risk analysis and offering construction project management scientific decision assistance.

The main contribution of this study is the proposal of a construction cost estimation model based on the Elman neural network combined with a GA, specifically:

Firstly, GA is applied to optimize the Elman neural network, utilizing GA to improve the weights and thresholds of the neural network, thereby enhancing the model's prediction accuracy and generalization ability. As a global search optimization tool, GA can avoid the problem of falling into local optimal solutions that is common in traditional training processes.

Secondly, by constructing a comprehensive index system and integrating it with the Elman neural network, a more accurate method for construction cost prediction is provided compared to traditional models. Furthermore, the model's applicability in complex construction projects is effectively improved through further optimization with GA.

Finally, the study focuses on the prediction of construction costs and proposes a new method for assessing cost overrun risks. Through the model's dynamic memory mechanism, it is possible to analyze the impact of historical data on future costs, identify potential risk

factors in advance, and provide decision support for project management.

2 Related work

In the construction industry, the accuracy of cost prediction is critical for the project's success. With the development of information technology, more and more researchers began to explore how to use advanced technical means to improve cost prediction accuracy. Mahmoodzadeh et al. forecasted the geological conditions, construction duration, and cost of tunnels using Gaussian Process Regression (GPR), Support Vector Regression (SVR), and decision tree models. Through 50% cross-validation to evaluate the model's performance, it was found that GPR was superior to SVR and decision trees in prediction accuracy. Hence, GPR was recommended to predict future tunnel projects' geological and construction time costs [10]. Alshboul et al. used an ML algorithm to predict the cost of green buildings, considering the influence of related attributes of soft and hard costs. The evaluation results showed that eXtreme Gradient Boosting (XGBoost) performed best in accuracy, followed by the deep neural network (DNN) and random forest (RF) [11].

These models could be used as decision-support tools for construction project managers and practitioners to promote the development of automation research in the green building industry.

Because neural networks can handle complicated nonlinear interactions, they have emerged as a potent tool for cost prediction problems. Pham et al. proposed an ML and optimization framework incorporating artificial neural networks (ANNs) and gradient boosting models to estimate construction costs and optimize costs under budget constraints rapidly [12]. Goodarizad et al. improved the accuracy of construction labor productivity models for concrete pouring operations through a hybrid model developed by combining ANN and Grasshopper optimization algorithms [13]. The study helped to improve project efficiency, increase labor productivity, and reduce costs. Kim et al. introduced an autoregressive integrated moving average (ARIMA)-ANN model to predict construction costs. They found that the model provided more accurate predictions in most cases, especially for long-term forecasting time limits, than standalone ARIMA or ANN models [14]. The main contents of the above research are summarized in Table 1.

Table 1: Summary of relevant research contents

| Model | Method | Dataset | Key results |
|---|--|--|--|
| GPR, SVR, Decision tree | ML method is used to predict tunnel geological conditions, construction period, and cost. The model's performance is evaluated by 5-fold cross-validation. | Tunnel project data | GPR has better prediction accuracy than SVR and decision tree. Meanwhile, it is recommended for geological and time cost prediction of future tunnel projects |
| XGBoost, DNN, and RF | By considering soft and hard cost attributes, ML methods are used to predict green building costs. | Green building-related data | XGBoost performs the best in prediction accuracy, with an accuracy of 0.96; This Is followed by DNN (0.91) and RF (0.87), which can provide decision support tools for the green building industry. |
| ANN, gradient boosting model | 13 ML regression algorithms are employed to estimate construction costs and optimize costs under budget constraints | Construction configuration dataset | ANN and gradient boosting algorithms perform the best, estimating construction costs and required resources with 99% accuracy in less than 1 second of training time, and reducing costs by 7% through optimization. |
| Hybrid model (ANN+Grasshopper algorithm) | The combination of ANN and Grasshopper optimization algorithm improves the labor productivity model of concrete pouring operation. | Labor productivity data for 24 commercial office complex projects under construction in Iran | The project efficiency is improved, labor productivity is increased, and costs are reduced |
| ARIMA-ANN model | The ARIMA model is integrated with ANN to predict construction costs. | National and city-level construction cost index | In most cases, especially in long-term forecasting, hybrid models have higher prediction accuracy than ARIMA or ANN models used alone. |

Although significant progress has been made in construction cost estimation, there remain substantial limitations in terms of generalization ability and overspending risk assessment. Specifically, many models rely on specific datasets, making it challenging to maintain prediction accuracy in new construction project scenarios. For instance, while models like GPR and XGBoost exhibit high prediction accuracy on particular datasets, their performance may decline significantly when applied to cross-dataset scenarios or when handling previously unseen complex situations. Existing research tends to focus more on cost prediction accuracy, with less emphasis on the quantification and identification of potential overspending risks. For complex construction projects, such models lacking risk assessment abilities could lead to delayed cost control decisions. To address these shortcomings, this study proposes a construction cost estimation model based on the Elman neural network, optimized with a GA. The GA enhances the model's global search capability by optimizing the initial weights and thresholds of the Elman neural network, thereby improving its prediction performance across different datasets and complex scenarios. The dynamic memory mechanism of the Elman neural network enables it to capture long-term dependencies in time-series data, allowing the analysis of cost trends and forecasting potential overspending risks. Moreover, by designing a comprehensive overspending risk index system, the model can quantitatively identify key factors that lead to cost deviations, providing a basis for risk prevention and control.

on the principles of comprehensiveness, scientificity, a combination of quantitative and qualitative methods, dynamics, and operability. These indexes are chosen from four aspects: architectural features, structural features, project positioning, and project environment. The method of literature analysis is used for this selection. The quantification of qualitative indexes is carried out [15-17]. In constructing the cost estimation and overspending risk index system, the selection of each index is based on its correlation with construction costs and overspending risk. For example, in the case of exterior wall decoration, significant differences in the price and construction techniques of different materials exist. Paint is relatively inexpensive, while materials such as stone and glass curtain walls are more costly and have longer construction periods, potentially increasing the overspending risk [18]. Similarly, the technical personnel level directly influences construction efficiency and quality. Low technical levels may lead to rework and delays, thus increasing both cost and the probability of overspending [19]. Architectural features such as floor area and standard floor height determine material usage and construction complexity, directly affecting the total project cost. Structural features, including the prefabrication rate and component differentiation, relate to the efficiency and cost control capacity of prefabricated construction. Project environmental factors, such as project management level and transportation distance, reflect the impact of management efficiency and logistics on cost. These indexes are validated through literature analysis and practical engineering experience, demonstrating their key role in cost control and overspending risk, thereby providing a theoretical foundation for the model's scientific and comprehensive nature. The finalized index system for assembly construction cost estimation prediction is outlined in Table 2.

3 Construction cost estimation model based on elman neural network

3.1 Construction cost estimation and construction of overspending risk index system

The study focuses on assembly buildings. The selection of indexes affecting the cost and overspending risk is based

Table 2: Construction cost estimation and overspending risk index system and assignment of values

| Primary index | Secondary index | Nature of the index | Assignment of qualitative index |
|------------------------|--------------------------|---------------------|---|
| Architectural features | Number of floors A1 | Quantitative index | - |
| | Building area A2 | Quantitative index | - |
| | Standard floor height A3 | Quantitative index | - |
| Structural features | Structure type A4 | Qualitative index | 1=internally cast and externally hung shear wall structure; 2=stacked shear wall structure; 3=assembled monolithic frame structure; 4=assembled monolithic shear wall structure |
| | Foundation type A5 | Qualitative index | 1 = independent foundation; 2 = pile foundation; 3 = raft slab foundation; 4 = pile raft foundation; 5 = box foundation |
| | Prefabrication rate A6 | Quantitative index | - |

| | | | |
|----------------------------|---|--------------------|--|
| | Component type A7 | Qualitative index | 1 = laminated panels/air conditioning panels/drift windows/enclosures; 2 = prefabricated stairs; 3 = beams/columns/shear walls |
| | Differentiation degree of components A8 | Quantitative index | - |
| Project positioning | Exterior wall decoration A9 | Qualitative index | 1=paint; 2=real stone paint; 3=glass curtain wall; 4=aluminum panel; 5=stone |
| | Interior wall decoration A10 | Qualitative index | 1=general plaster; 2=plaster; 3=large white; 4=latex paint; 5=wall tiles; 6=wallpaper |
| | Ground engineering A11 | Qualitative index | 1=concrete topping; 2=ordinary tiles; 3=flooring; 4=premium tiles |
| | Door and window type A12 | Qualitative index | 1=plastic steel window + steel door; 2=aluminum alloy window + steel door; 3=plastic steel window + fire door; 4=aluminum alloy window + fire door |
| Project environment | Technical personnel level A13 | Qualitative index | 1=excellent; 2=good; 3=medium; 4=poor |
| | Project management level A14 | Qualitative index | 1=excellent; 2=good; 3=medium; 4=poor |
| | Transportation distance A15 | Quantitative index | - |

In the above index system, the three indexes of architectural features are directly related to the building's physical size and construction complexity, affecting material costs and labor requirements. These in turn affect cost control and the risk of overspending. The indexes of structural features determine the structural stability and construction methods, significantly impacting material selection and supply chain management, thus correlating with the overspending risk. Project positioning includes qualitative indexes such as exterior and interior wall decorations, ground engineering, and window and door types. These choices affect the building's aesthetics and functionality while leading to increased costs, which may increase overspending risk if costs are not properly

controlled. Moreover, indexes in the project environment reflect the efficiency of project management and the impact of external conditions on costs, which are key factors in cost control and risk management. This system helps to forecast costs more accurately while identifying and controlling factors that may lead to overspending.

In the above index system, the priority of each index varies depending on its impact on costs and overspending risks. To ensure that the indicator system can comprehensively and scientifically reflect the risk of cost overruns, the Analytic Hierarchy Process is used to assign weights to each index. The results are exhibited in Table 3.

Table 3: Index system weight

| Primary index | Weight of primary index | Secondary index | Final weight |
|-------------------------------|-------------------------|---|--------------|
| Architectural features | 0.162 | Number of floors A1 | 0.054 |
| | | Building area A2 | 0.054 |
| | | Standard layer height A3 | 0.054 |
| Structural features | 0.409 | Structure type A4 | 0.128 |
| | | Foundation type A5 | 0.073 |
| | | Prefabrication rate A6 | 0.053 |
| | | Component type A7 | 0.069 |
| | | Differentiation degree of components A8 | 0.086 |
| Project positioning | 0.290 | Exterior wall decoration A9 | 0.044 |
| | | Interior wall decoration A10 | 0.068 |
| | | Ground engineering A11 | 0.121 |
| | | Door and window type A12 | 0.057 |
| Project environment | 0.139 | Technical personnel level A13 | 0.073 |
| | | Project management level A14 | 0.046 |

| | | | |
|--|--|-----------------------------|-------|
| | | Transportation distance A15 | 0.020 |
|--|--|-----------------------------|-------|

In Table 3, structural features hold the highest weight among the primary indexes, accounting for 40.9%, indicating their most significant impact on both construction costs and overspending risk. Among these, A4 and A8 have relatively higher weights of 0.128 and 0.086, respectively, reflecting the crucial role of building structure complexity and differentiation in cost control. The project positioning index ranks second, accounting for 29.0%, with A11 having the highest weight of 0.121, emphasizing its importance in construction decoration costs. The weights for architectural features and project environment are relatively lower. However, among the secondary indexes, A13 and A2 stand out with weights of 0.073 and 0.054, respectively, highlighting their influence on construction efficiency and total cost prediction. This weight allocation method enables the index system to more scientifically reflect the contribution of various factors to cost and overspending risk, providing a solid foundation for subsequent model predictions and risk analysis.

3.2 Elman neural network modeling analysis

The Elman neural network's key feature is the incorporation of a context layer, which preserves the hidden layer's state from a previous time step [20]. This enables the Elman network to process time-series data, capturing the dynamics of the input data and the underlying temporal relationships, making it suitable for time-dependent data prediction tasks such as construction costs. The network creates a short-term memory mechanism by feeding past information back to the current moment, which enhances its ability to model nonlinearities in dynamically changing processes. Unlike traditional feed-forward neural networks, the Elman network has feedback connections between the hidden and context layers. These feedback signals allow the network to retain information from previous states, providing valuable contextual input for subsequent computations [21, 22]. Figure 1 depicts the Elman neural network's basic structure.

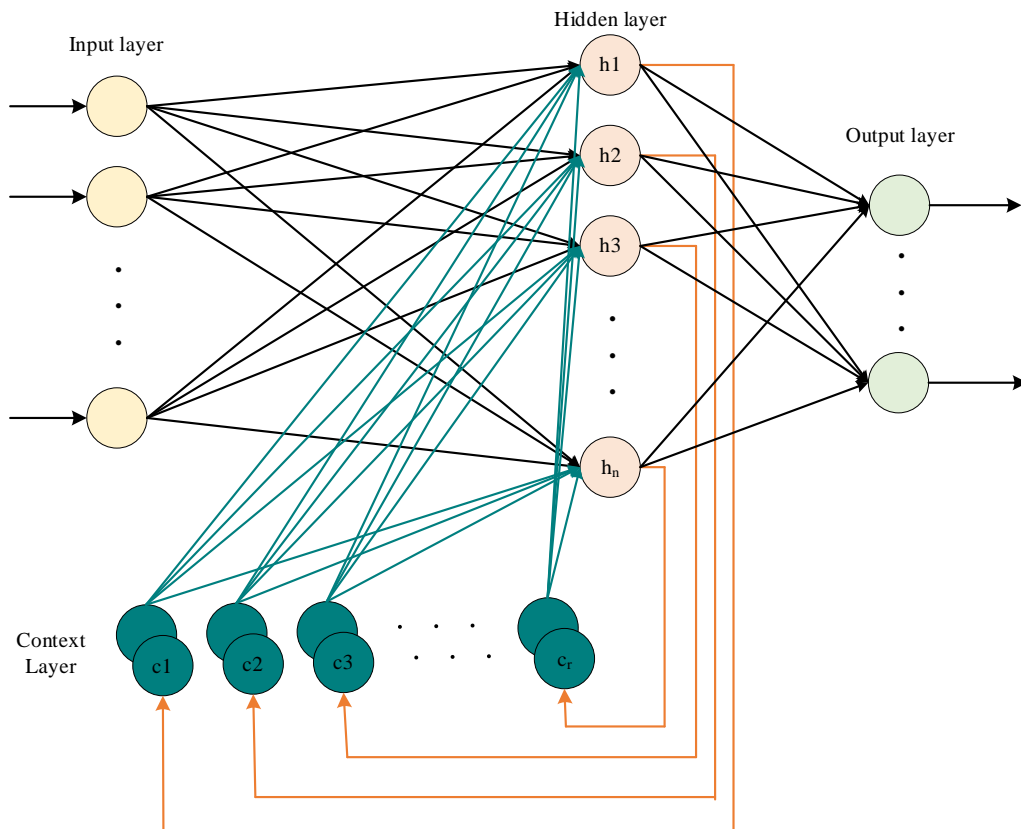


Figure 1: Schematic diagram of Elman network structure

The core principle of the Elman network is as follows. First, the output vector $y(t)$ of the network is obtained from the output vector $h(t)$ of the implicit layer through the nonlinear transformation function $g(*)$ of the output layer with the expression (1):

$$y(t) = g(w_{hy}w_{cj}^y h(t)) \tag{1}$$

w_{hy} denotes the weight matrix between the hidden and output layers. Secondly, the output $h(t)$ of the implicit layer is obtained from the current input $v(t - 1)$ and the output $c(t)$ of the context layer through the

nonlinear transformation function $f(*)$ of the implicit layer with the expression (2):

$$h(t) = f(w_{xh}v(t - 1) + w_{ch}c(t)) \quad (2)$$

w_{xh} refers to the weight matrix from the input to the hidden layer. w_{ch} denotes the weight matrix from the takeover layer to the hidden layer. Finally, the output $c(t)$ of the take-on layer is the output $h(t - 1)$ of the implicit layer at the previous time step, that is (3):

$$c(t) = h(t - 1) \quad (3)$$

This structure allows the Elman network to capture the temporal dynamics of the input data. For construction cost estimation, it means that the network can consider the impact of historical cost data on current cost estimates, thus improving the accuracy of the predictions.

Furthermore, the computational flow of the Elman network is suggested in Figure 2.

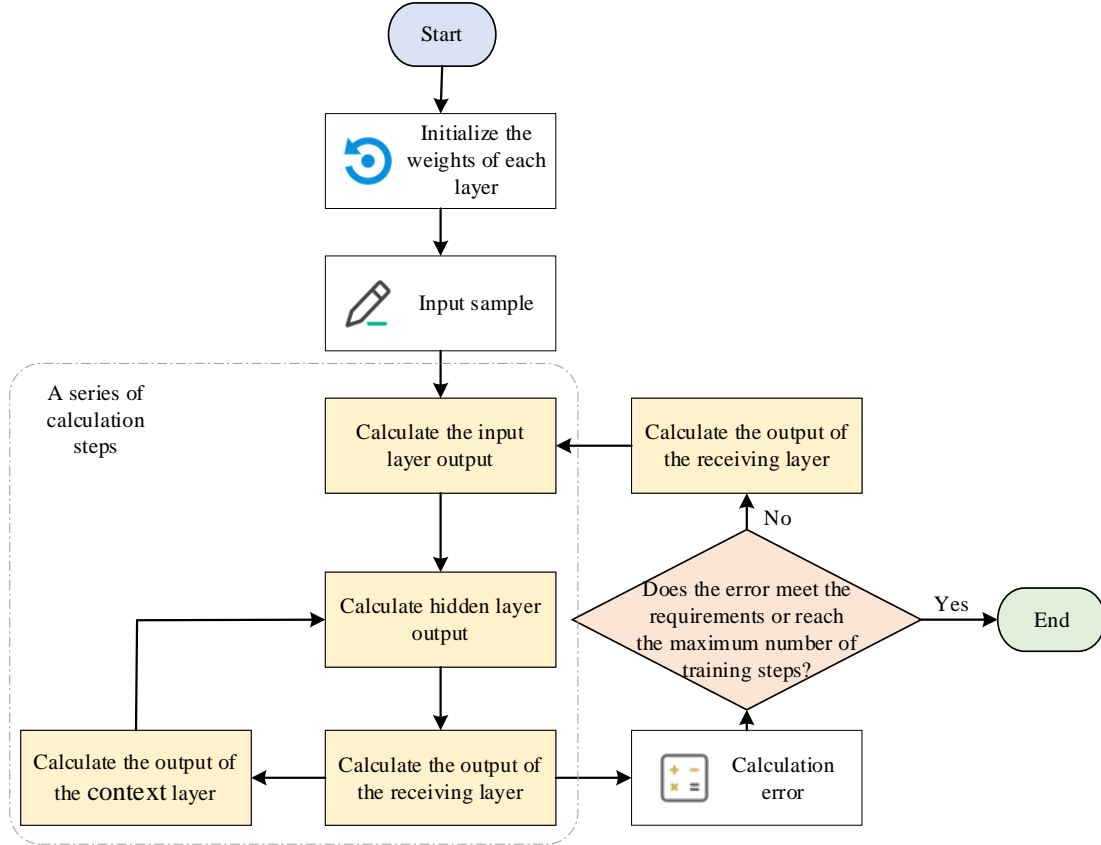


Figure 2: Elman network computational flow

In Figure 2, the network initializes the weights of each layer as a necessary preparation before training starts. The initial setup of these weights significantly impacts the learning effectiveness and overall performance of the network. Network learning is then built on the input samples, which include past construction project cost data and other pertinent features. The outputs of the input, hidden, and output layers are then computed sequentially. Meanwhile, after obtaining the output of the hidden layer, the output of the context layer is further computed. In this step, the current output of the hidden layer is used as the input for the context layer in the next time step. This step is the key to the short-term memory mechanism of the Elman network, allowing it to retain information from previous states while processing sequential data. The output layer error is determined by comparing the actual cost data with the network's predicted outputs, following the computation of outputs across all layers. A critical element of supervised learning, this error computation (denoted as E) provides the network with feedback for adjusting its parameters. Lastly, the error E is utilized to check if the maximum number of training steps has been completed or if the predefined requirements are met. If the

error E does not decrease sufficiently, the training cycle continues, with the weights being adjusted to reduce the prediction error. This process is repeated until the network performs adequately or the training reaches the set number of iterations.

In the above step, the error E is used to measure the difference between the predicted output of the network, $y(t)$, and the desired output as $\hat{y}(t)$, calculated as (4):

$$E = \frac{1}{2}(y(t) - \hat{y}(t))^T (y(t) - \hat{y}(t)) \quad (4)$$

To adjust the weights, the partial derivatives of the error E with respect to the weights need to be calculated. The partial derivatives of the weights w_{ji}^y for the output layer are (5):

$$\frac{\partial E}{\partial w_{ji}^y} = -(\hat{y}_{d,i}(t) - y(t)) \frac{\partial y_i(t)}{\partial w_{ji}^y} = -(\hat{y}_{d,i}(t) - y(t)) g'_j(*) x_i(t) \quad (5)$$

w_{ji}^y refers to the weight connecting the i th input unit and the j th output unit; $g'_j(*)$ represents the derivative of the activation function of the output layer; $x_i(t)$ denotes the output of the i th input unit at time t . Let $\varphi_j^0 = (\hat{y}_{d,i}(t) - y(t)) g'_j(*)$, so (6):

$$\frac{\partial E}{\partial w_{ji}^y} = -\varphi_j^0 x_i(t), i = 1, 2, \dots, m; j = 1, 2, \dots, n \quad (6)$$

m is the number of neurons in the input layer and n is the number of neurons in the hidden layer.

Taking E as the partial derivative of the input layer weight w_{ji}^x , it can get (7):

$$\frac{\partial E}{\partial w_{ji}^x} = \frac{\partial E}{\partial x_i(t)} \frac{\partial x_i(t)}{\partial w_{ji}^x} = \sum_{i=1}^m (-\varphi_j^0 w_{ji}^x) f'_i(*) v_q(t-1) \quad (7)$$

$f'_i(*)$ denotes the derivative of the hidden layer activation function. Let $\varphi_j^h = \sum_{i=1}^m (-\varphi_j^0 w_{ji}^x) f'_i(*)$, L, then get (8):

$$\frac{\partial E}{\partial w_{ji}^x} = -\varphi_j^h v_q(t-1), i = 1, 2, \dots, m; j = 1, 2, \dots, n; q = 1, 2, \dots, r \quad (8)$$

r is the number of neurons in the splice layer.

The partial derivative of the connection weight w_{ji}^c is obtained (9):

$$\frac{\partial E}{\partial w_{ji}^c} = \sum_{i=1}^m (-\varphi_j^0 w_{ji}^x) \frac{\partial x_i(t)}{\partial w_{ji}^c}, l = 1, 2, \dots, n; j = 1, 2, \dots, n \quad (9)$$

According to the chain rule (10):

$$\frac{\partial x_j(t)}{\partial w_{ji}^c} = \frac{\partial}{\partial w_{ji}^c} f_j(\sum_{i=1}^n w_{ji}^c x_{c,i}(t) + \sum_{i=1}^r w_{ji}^x v_i(t-1)) = f'_j(*) x_{c,i}(t) + \sum w_{ji}^y \frac{\partial x_{c,i}(t)}{\partial w_{ji}^y} \quad (10)$$

The dependence of $x_c(t)$ on the connection weight w_{ji}^y is ignored, and the following results are obtained (11) and (12):

$$\frac{\partial x_j(t)}{\partial w_{ji}^c} = f'_j(*) x_{c,i}(t) \quad (11)$$

$$f'_j(*) x_{c,i}(t) = f'_j(*) x_i(t-1) + \alpha * f'_j(*) x_{c,i}(t) \quad (12)$$

α refers to the forgetting factor. By substituting equation (12) into equation (11), it can obtain (13):

$$\frac{\partial x_j(t)}{\partial w_{ji}^c} = f'_j(*) x_i(t-1) + \alpha * \frac{\partial x_j(t-1)}{\partial w_{ji}^c} \quad (13)$$

Elman's equation (14)-(18) is derived from $\Delta W = -\eta \frac{\partial E}{\partial W}$:

$$\Delta w_{ji}^y = \eta \varphi_j^0 x_j(t), i = 1, 2, \dots, m; j = 1, 2, \dots, n \quad (14)$$

$$\Delta w_{jq}^c = \eta \varphi_j^h v_q(t-1), j = 1, 2, \dots, n; q = 1, 2, \dots, r \quad (15)$$

$$\Delta w_{jl}^x = \eta \sum_{i=1}^m (\varphi_j^0 w_{ji}^x) \frac{\partial x_i(t)}{\partial w_{ji}^x} \varphi_j^0 x_j(t), j = 1, 2, \dots, n; l = 1, 2, \dots, n \quad (16)$$

η is the learning rate. Meanwhile,

$$\varphi_j^0 = (\hat{y}_{d,i}(t) - y(t)) g'_j(*) \quad (17)$$

$$\varphi_j^h = \sum_{i=1}^m (-\varphi_j^0 w_{ji}^x) f'_i(*) \quad (18)$$

Through this calculation process, the Elman network can gradually learn the complex relationship between building cost data and complete cost prediction. This dynamic learning and forecasting mechanism makes the Elman network perform well in dealing with time series forecasting problems such as construction cost estimation. The pseudocode for the Elman model is illustrated in Figure 3.

Algorithm: Elman Neural Network

Input:

- Training data
- Learning rate
- Maximum iterations

Initialization:

- Randomly initialize weights
- Set initial context layer to zero

Training:

Repeat until convergence or maximum iterations:

1. Compute hidden layer output
2. Update context layer
3. Compute network output
4. Calculate error
5. Backpropagate and update weights

Prediction:

For each input in test data:

1. Compute hidden layer output
2. Update context layer
3. Compute final output

Figure 3: The pseudocode for the Elman model

3.3 Optimization of the Elman model based on GA

Although the Elman neural network has remarkable advantages in processing time series data, its performance is highly dependent on the initial weight settings and the choice of network structure. In addition, the Elman network is easily affected by local minimum, which can lead to suboptimal solutions and negatively impact prediction accuracy and generalization ability [23]. To overcome these limitations, GA is introduced to optimize the Elman model. Darwin's theory of natural selection and the global search principle of biogenetics serve as the foundation for GA, an optimization algorithm designed to mimic the natural evolution process. Biological evolution mechanisms, including natural selection, genetic variation, and crossover, are simulated by GA, which is extensively used to tackle complicated combinatorial optimization problems by gradually improving the quality of solutions. GA has strong global search ability and adaptability, and can effectively deal with optimization problems under high dimensional, nonlinear, and complex constraints [24]. The basic idea of GA is to simulate natural selection and genetic mechanisms by operating a population composed of multiple individuals to produce better solutions. Although GA possesses global search capabilities and strong adaptability, there are certain limitations in its optimization process. GA may encounter issues of high computational complexity and time costs when dealing with large-scale datasets. Additionally, the

convergence speed of GA can be slow, especially in large search spaces, where there is a risk of premature convergence or falling into local optimal solutions [25]. The implementation steps of GA are displayed in Figure 4.

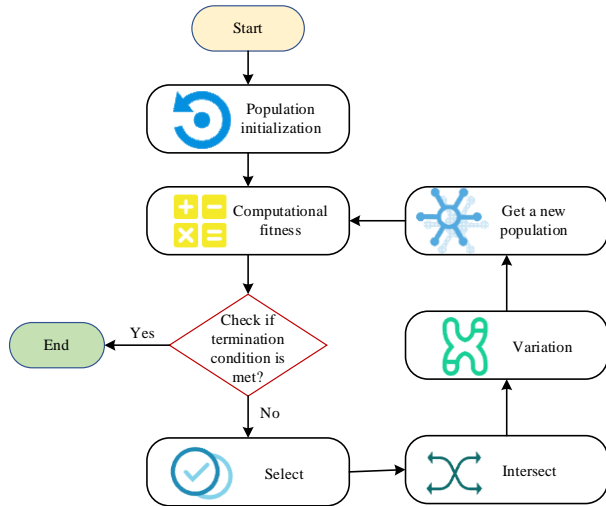


Figure 4: GA implementation process

This study uses the GA to optimize the adjustment of Elman network weights and thresholds, and the specific steps are as follows [26, 27].

(1) Population initialization. Several initial individuals are randomly generated in the solution space, and each individual corresponds to a set of potential Elman network weights and thresholds. Each individual can be regarded as the coding form of Elman network parameters (real number coding), including the connection weights between input and hidden layers, hidden and output layers, and the threshold of each neuron.

(2) Fitness calculation. According to the performance index of the Elman network (for example, the mean square error of construction cost estimation), the fitness of each individual is evaluated. The network corresponding to the individual performs better on a given task the higher the fitness.

(3) Selection of the operation. Using probability techniques like roulette wheel selection, the fittest

members of the current population are chosen to go into the next generation based on their fitness values. This step imitates the natural selection process of "survival of the fittest" in biology.

(4) Cross operation. Individuals are randomly paired from the selected ones and undergo a single-point crossover operation according to a set crossover probability (0.6). This involves randomly selecting a position in the chromosome and exchanging the gene segments before and after that position, generating new combinations of weights and thresholds. This method improves search efficiency by exploring different parameter combinations.

(5) Mutation operation. A small probability (0.2) is used to randomly mutate certain genes of the selected individuals. The specific method is to add a random disturbance that follows a normal distribution (e.g., with a mean of 0 and a standard deviation of 0.1) to the original weights or thresholds. Thus, it can increase the diversity of the population and avoid local optimal solutions.

(6) Termination conditions. For one thing, the algorithm automatically stops when it reaches the preset maximum number of iterations (200 times). For another, if the optimal fitness value of the population does not improve by more than a predetermined threshold (0.001) over a continuous number of generations (20), it is considered that the algorithm has converged. In addition, the optimization process is terminated early. By introducing these clear stopping criteria, the stability of the optimization process can be effectively ensured, while also enhancing the applicability and reliability of the algorithm in practical problems.

Through the aforementioned optimization process, GA can effectively adjust the weights and thresholds of the Elman network, improving the model's generalization ability and prediction accuracy. The rationality of parameter settings is determined through multiple experimental tests. Meanwhile, the specific implementation of crossover and mutation ensures a high degree of repeatability in the study, providing an effective modeling tool for complex construction cost estimation tasks.

Figure 5 shows the calculation flow of the finally formed GA-Elman model based on GA.

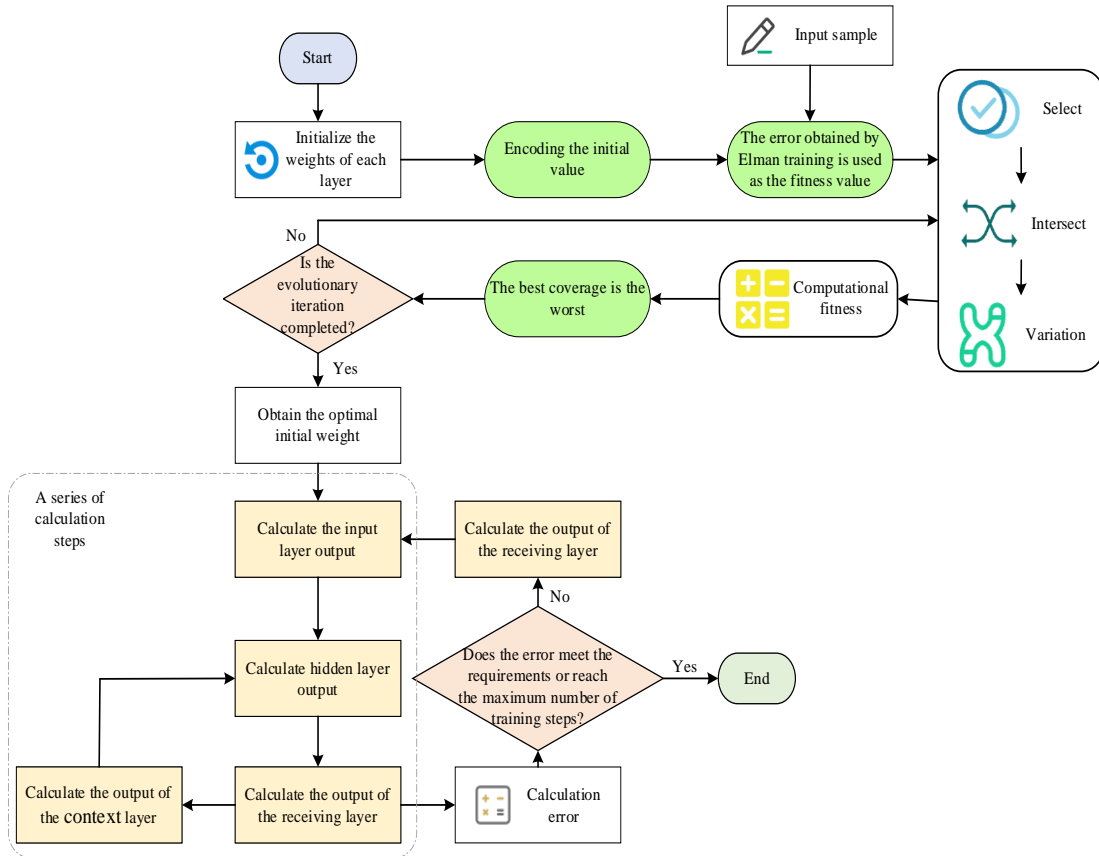


Figure 5: Calculation flow of GA-Elman model

The GA optimization of the Elman neural network can reduce the probability of the model reaching local optima, and enhance the network's global search ability. Meanwhile, it can accelerate the convergence speed of the training process and improve the model's prediction accuracy. This is especially important for complex construction cost estimation tasks. Especially when faced with time-related data, the optimized GA-Elman network can better capture the dynamic characteristics of data and realize more accurate cost estimation and risk prediction.

3.4 Application of cost estimation model in overspending risk

In the cost management of construction projects, the assessment and control of overspending risk is a crucial link. The assessment of overspending risk relies on the accuracy of cost estimation while requiring scientific quantification of risk factors and their weights. The GA-Elman model can accurately capture the time series characteristics of cost data through dynamic memory mechanisms, offering vital support for the quantitative assessment of overspending risk. Firstly, the assessment of overspending risk is based on the cost deviation rate p , and the degree of risk is quantified by the deviation between the model's predicted value c' and the actual cost value c . The specific calculation reads (19):

$$p = \frac{|c - c'|}{c'} \times 100\% \quad (19)$$

In this context, the higher the deviation rate, the greater the overspending risk. Based on this deviation rate, the risk can be classified into three levels: low, medium,

and high, providing decision-makers with a more intuitive risk assessment index.

Furthermore, the model quantifies the key risk factors through a comprehensive index system. The index system designed in this study encompasses four major dimensions: architectural features, structural features, project positioning, and project environment. Within each dimension, specific indexes are assigned different weights to reflect their relative importance in contributing to cost overruns. For instance, in the architectural features dimension, the "number of floors" and "building area" directly influence material and labor costs, with their weights determined by principal component analysis. In contrast, in the project environment dimension, "management level" and "technical personnel level" are quantified using fuzzy comprehensive evaluation methods. The distribution of risk factor weights follows (20):

$$w_i = \frac{v_i}{v} \quad (20)$$

w_i represents the weight of the i th risk factor, with a value range of 0 to 1 and a total weight of 1; v_i refers to the contribution of the i th index to the total deviation; v denotes the total deviation. The GA-Elman model can identify and predict the primary risk factors leading to overspending through historical data. For example, the model can use retrospective analysis to determine that material price fluctuations contribute 35% to cost deviations, construction delays account for 25%, design changes contribute 20%, and other factors make up 20%. This detailed quantitative analysis helps managers pinpoint key risk sources and provides data support for formulating targeted risk control strategies.

Additionally, the GA-Elman model simulates the impact of different cost control strategies on overspending risk. For instance, in the case of significant material price fluctuations, the model can simulate cost trends for diverse procurement strategies (such as bulk purchasing in advance or phased procurement) and assess the mitigation effects of each strategy on overspending risk. This data-driven simulation analysis offers project managers a scientific decision-making tool.

To sum up, the GA-Elman model in overspending evaluation provides intuitive risk levels through the quantification of cost deviations. Meanwhile, it offers a systematic approach to risk identification, assessment, and control through the weight allocation to key risk factors and simulation analysis. By applying this model in-depth, project managers can remarkably improve risk management efficiency, reduce economic losses caused by overspending, and ultimately enhance the construction projects' cost-effectiveness and success rate.

4 Model Performance verification

4.1 Data source and experimental design

To ensure the universality and representativeness of the experiment, data are collected from multiple sources, ensuring the diversity and reliability of the data. The social and economic development level of each region and the number of prefabricated buildings built are comprehensively considered. The basic data are obtained from professional platforms such as the China Prefabricated Building Market Analysis Report, Prefabricated Building Network, and Zhongce Big Data Website. Additionally, data from 45 groups of prefabricated building projects in cities such as Beijing, Tianjin, Hebei, and Shenyang over the past four years are collected. These data cover many dimensions, such as architectural features, structural features, project positioning, and project environment, offering rich information for model training and testing. Taking the indexes A1-A3 of architectural features as an example, the variance analysis of these data is detailed in Table 4.

Table 4: Variance analysis of architectural feature indexes

| Difference source | Sum of Squares | Degrees of Freedom | Mean Square | F | P-value | F crit |
|-------------------|----------------|--------------------|---------------|--------|---------|--------|
| Row | 3,417,030,830 | 44 | 77,659,791 | 1.000 | 0.488 | 1.515 |
| Column | 4,022,937,273 | 2 | 2,011,468,636 | 25.902 | 0.000 | 3.100 |
| Error | 6,833,762,444 | 88 | 77,656,391 | | | |

Table 4 shows significant mean differences ($P < 0.05$) among variables A1, A2, and A3, while the differences between samples are not significant. This indicates that different samples have a relatively small impact on the results of variance analysis. These data can more comprehensively illustrate the distribution characteristics of architectural feature data, providing data support for model prediction. To enhance the model's generalization ability, the gathered data are normalized to remove the impact of varying dimensions and ordering. Specifically, the Min-Max normalization method is adopted to map the data values of each index to the interval $[0, 1]$, and the normalization equation is as follows (21):

$$X' = \frac{X - X_{min}}{X_{max} - X_{min}} \quad (21)$$

X is the original data; X_{min} and X_{max} are the minimum and maximum values of the index, respectively. Through this method, the differences in dimensions and magnitudes between different indicators have been eliminated, ensuring the stability and accuracy of the model during training and testing. The training set comprises 36 sets of data; The test set contains 9 sets of data, which are randomly selected from the dataset and arranged in a 4:1 ratio. Furthermore, to comprehensively evaluate the performance and reliability of the model, this study further adopts the k-fold cross-validation technique ($k=5$) based on the division of training and testing data. By partitioning the dataset k times to ensure that each subset participates in training and validation, the potential random errors caused by a single partition are effectively reduced. In addition, the stability and credibility of the

model evaluation results are improved. The experimental setup and parameter values are shown in Table 5.

Table 5: Experimental environment and parameter setting

| Hardware/parameter name | Parameter/value |
|------------------------------|--------------------|
| Operating system | Windows10 |
| CPU | AMD R7-5800H |
| Basic frequency | 3.2 GHz |
| Display card | RTX3060 |
| Memory | 16 GB |
| Hard disc | 512 G SSD |
| Input layer node | 15 |
| Output layer node | 1 |
| Hidden layer node | 10 |
| Maximum number of iterations | 200 |
| Error tolerance | 1×10^{-5} |
| Evolutionary algebra | 20 |
| Population size | 10 |
| Cross probability | 0.6 |
| Mutation probability | 0.2 |

Relative Error (RE) and Mean Absolute Percentage Error (MAPE) are used as evaluation indexes to evaluate the accuracy of prediction results. The calculation equations of them are (22) and (23):

$$RE = \frac{y'_i - y_i}{y'_i} * 100\% \quad (22)$$

$$MAPE = \frac{1}{N} \sum_{i=1}^n \frac{|y_i - y'_i|}{y_i} \quad (23)$$

N represents the number of samples. y_i and y'_i refer to the predicted and actual values. In the cost estimation model, REP measures the difference between the predicted and actual costs to evaluate the model's prediction performance. MAPE index can directly reflect the RE between the actual and predicted values of the model, and it is an important index to measure the model's prediction performance.

4.2 Test results of the GA-Elman model

Firstly, the GA-Elman model is trained, and its training result in the training set is presented in Figure 6.

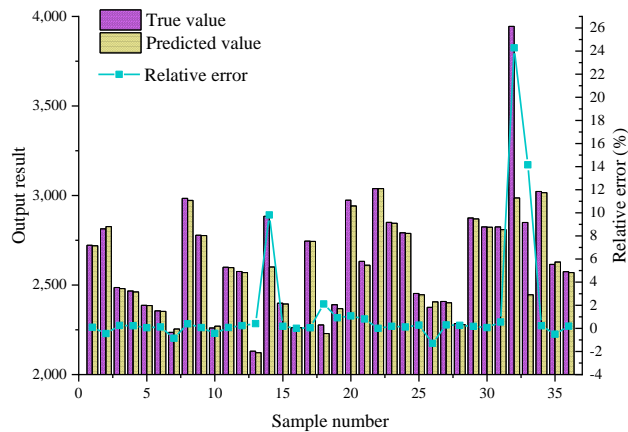


Figure 6: Training results of the GA-Elman model in the training set

Results in Figure 6 demonstrate that the GA-Elman model has good prediction accuracy. This is because the predicted values for most samples are extremely close to the true values and the RE percentage is typically less than 1%. However, there are also some samples with large prediction errors, such as Samples 14 and 32, with RE percentages as high as 9.816% and 24.284%. The reasons for these issues may be attributed to several factors. Firstly, the data characteristics of these samples may significantly deviate from the overall distribution of the training set, such as abnormal fluctuations in key factors like material prices, construction conditions, or design complexity. For instance, Sample 32 may have actual costs that far exceed the model's predictions due to the use of certain specific processes or unexpected construction delays. Secondly, the model may exhibit limitations in handling rare features in small samples, especially when these features are not adequately represented in the training data, making it difficult for the model to capture their nonlinear relationships. Additionally, the data preprocessing process may not have eliminated the effects of noise or outliers, which could also amplify errors. To address the aforementioned issues, the following approaches can be taken. Firstly, it is necessary to optimize data preprocessing methods by employing techniques such as denoising and smoothing to improve data quality. Meanwhile, the detection and handling of outliers are strengthened to reduce the noise interference on the model. Secondly, the sample diversity of the training dataset is expanded, particularly for samples with rare or abnormal features, by increasing the proportion of related data,

thereby enhancing the model's ability to learn nonlinear relationships. Moreover, integrating learning methods or hybrid model structures can be introduced to combine the advantages of multiple algorithms and improve the model's generalization ability. Lastly, for key features such as material prices and construction conditions, targeted feature engineering strategies can be designed to ensure that the model can more accurately capture their impacts, thus reducing the occurrence of extreme errors.

Taking the Elman network, RNN, and SVR as the benchmark model, the test set is tested on the GA-Elman and benchmark models, respectively, and the results are revealed in Figure 7.

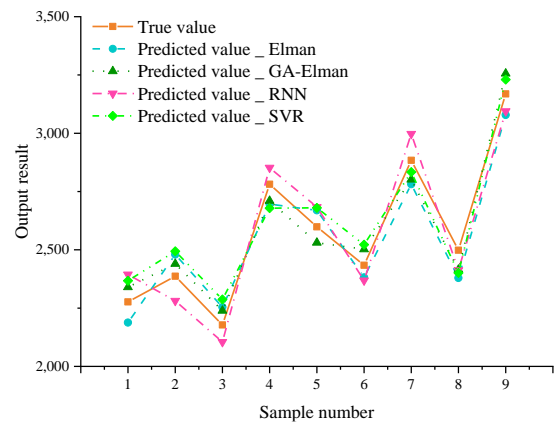


Figure 7: Comparison between the GA-Elman model and benchmark model

On most test samples, the predicted value of the GA-Elman model in Figure 7 is more similar to the true value. The maximum differences between the predicted and actual results for the Elman network, RNN, and SVR are 118.99, 117.65, and 102.94, respectively. The GA-Elman model's maximum difference between the predicted and true values is 87.21. These results show that the GA-Elman model optimized by GA has higher prediction accuracy and robustness in construction cost estimation, thus verifying the effectiveness of GA in neural network weight optimization.

4.3 Comparison of cost estimation results before and after Elman model optimization

To further compare the cost estimation results before and after the optimization of the Elman model, the difference between the predicted and true value and the RE of the four models are calculated, as denoted in Figure 8.

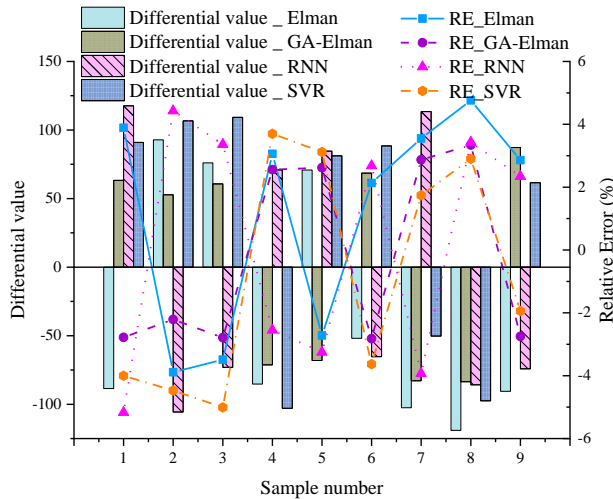


Figure 8: Analysis of cost prediction results of four models

In Figure 8, the differences and REs of the GA-Elman model across all test samples are generally lower than those of the Elman model. The mean absolute difference between the predicted and actual values for the GA-Elman model is 70.93, while for the Elman network, RNN, and SVR, they are 86.38, 87.83, and 87.63, respectively. In some samples, the GA-Elman model still exhibits relatively large errors. The main reasons for these larger errors are twofold. First, data irregularity. For instance, Sample 8 may have been affected by drastic fluctuations in material prices or abnormal construction environments, leading to actual costs significantly higher than the model's predictions. However, these exceptional situations are not adequately represented in the training data. Second, model limitations. The GA-Elman model has enhanced its ability to capture nonlinear features through parameter optimization by GA. Nevertheless, it may still be insufficiently responsive to the dynamic changes of certain key influencing factors, such as unexpected design changes or construction delays. Meanwhile, the calculated MAPE for the GA-Elman model is 2.75%, which is significantly reduced compared to the Elman model's 3.37%. The MAPEs for RNN and SVR are 3.46% and 3.45%, respectively, higher than that of the GA-Elman model. This further demonstrates the effectiveness of GA in optimizing neural network parameters and improving prediction accuracy. These results show that GA-Elman model is more accurate in capturing the complex relationship of construction cost data, thus providing more reliable support in cost estimation and overspending risk assessment of construction projects.

In addition, the training time of the GA-Elman and Elman models is compared, and the results are listed in Table 6.

Table 6: Comparison of training time between GA-Elman and Elman models

| Model | Training dataset size (number of samples) | Training time (seconds) |
|----------------|---|-------------------------|
| Elman model | 100 | 12.36 |
| | 500 | 56.47 |
| | 1,000 | 115.82 |
| GA-Elman model | 100 | 18.75 |
| | 500 | 72.93 |
| | 1,000 | 142.68 |

Table 6 indicates that the training time of the GA-Elman model is slightly higher than that of the traditional Elman model, primarily due to the additional optimization step introduced by the GA. However, this extra computational cost is justified, as the GA-Elman model optimizes the network's initial parameters and weights through GA, significantly improving both prediction accuracy and generalization ability. Specifically, when the sample size is small (e.g., 100 samples), the training time of the GA-Elman model is 18.75 seconds, only 6.39 seconds longer than the Elman model. When the sample size increases to 1,000, the training time becomes 142.68 seconds, which is 26.86 seconds longer than the Elman model. This increase in training time is acceptable in light of the improvements in prediction performance.

From both a construction and economic perspective, the improvements made by the GA-Elman model are significant. In construction management, accurate cost forecasting is crucial for budget control and risk mitigation. The GA-Elman model's high prediction accuracy (with a MAPE of only 2.75%) enables it to capture the complex nonlinear relationships in construction costs, thus providing project managers with more reliable decision support. This capability is especially beneficial for large and complex projects, as it helps reduce overspending risks and delays due to budget miscalculations. Additionally, by accurately assessing key influencing factors (such as material prices and construction conditions), the model helps managers identify potential risks earlier, allowing for timely adjustments in construction plans and financial allocations.

From an economic perspective, the application of the GA-Elman model in budget optimization remarkably improves resource allocation efficiency. Compared to the traditional Elman model and other benchmark models, the GA-Elman model offers a clear advantage in effectively reducing unnecessary financial waste and optimizing financial planning. For example, for cost-sensitive samples (such as Samples 14 and 32), there is still some error. However, the model provides managers with a cost estimate closer to the actual values, laying a foundation for reasonable financial resource distribution and cash flow control. Moreover, the GA-Elman model's ability to identify and quantify overspending risk allows enterprises

to develop more scientifically-based long-term financial strategies, thereby reducing the economic losses caused by uncontrollable costs.

In conclusion, the GA-Elman model has considerable potential in construction cost estimation and economic risk management. It enhances the intelligence level of construction management while providing a reliable tool for budget optimization and cost control. The model contributes positively to lean management and improved economic efficiency in the construction industry.

4.4 Discussion

Compared to the existing models summarized in Table 1, the proposed GA-Elman model demonstrates significant advantages in construction cost estimation and overspending risk assessment. In contrast to models such as GPR and XGBoost, the GA-Elman model is better suited for handling dynamic changes in time series data. For instance, while GPR exhibits high accuracy in predicting tunnel geological conditions, its sensitivity to data scale can lead to decreased computational efficiency when dealing with large-scale complex construction projects. In comparison, the GA-Elman model, by optimizing weights and thresholds through GA, can process large-scale data more efficiently while fully capturing dynamic changes, thus enhancing the model's applicability.

The comparison with ANNs and gradient boosting models indicates that although these models perform well in rapid construction cost estimation, they lack capability in risk assessment. For example, the gradient boosting model primarily focuses on cost optimization and cannot effectively identify key risk factors leading to overspending. In contrast, the GA-Elman model can predict costs and identify key drivers of overspending risks (such as fluctuations in material prices and construction delays) through its dynamic memory mechanism. As a result, it can provide project managers with more targeted decision support.

Compared to hybrid models such as ANN combined with the Grasshopper algorithm and ARIMA-ANN models, the GA-Elman model performs better in long-term forecasting and modeling complex data relationships. Although the ARIMA-ANN model has certain advantages in long-term construction cost estimation, its ability to capture nonlinear features is limited. The GA-Elman model, by optimizing network structure through the global search capability of GA, can better model nonlinear and temporal characteristics. Meanwhile, it can achieve superior prediction accuracy in practical tests, with the MAPE reduced to 2.75%.

In summary, the GA-Elman model outperforms existing models in terms of cost prediction accuracy, overspending risk assessment ability, and adaptability to complex data. Thus, it offers an innovative solution for construction cost management and significant practical guidance for budget control and risk management in complex engineering projects.

5 Conclusion

This study analyzes the application of the GA-Elman model in construction cost estimation and overspending risk analysis by constructing a construction cost estimation model based on the Elman network and optimizing the model with GA. It verifies the performance of the model through experiments. The conclusions are as follows. (1) The GA-Elman model's high prediction accuracy is demonstrated by the fact that, on the training set, the predicted value on most samples is very near to the true value and the RE percentage is typically within 1%. (2) When compared to the Elman network, the GA-Elman model's projected value is closer to the actual value, and on all test samples, the model's difference and RE are typically smaller than those of the Elman model. (3) The GA-Elman model's MAPE is 2.75%, a considerable decrease from the Elman model's 3.37%. It further proves the effectiveness of GA in optimizing neural network parameters and improving prediction accuracy. In short, by optimizing GA, the GA-Elman model increases the ability to detect possible overspending, which is crucial for efficient cost control and budget management, in addition to improving the accuracy of cost prediction. Although this study has made some progress in construction cost estimation and overspending risk assessment, there are still some limitations. First, the robustness of the model needs to be enhanced, as extreme errors occurring on specific data samples indicate insufficient stability. Second, the study only selects certain regions and prefabricated buildings, and the limitation of the sample range may affect the model's generalization ability, making it difficult to apply to other regions or different building types. Additionally, there may be biases in data selection, such as differences between urban and rural projects or the impact of various construction technologies (e.g., traditional construction versus modern building technologies). These factors could significantly affect the model's applicability and accuracy. Future research should consider more comprehensive data collection, covering a wider range of regions, building types, and different construction technologies, to avoid biases caused by data limitations, thereby enhancing the model's generalization ability and adaptability. At the same time, more advanced data preprocessing techniques and algorithm optimization methods can be explored to improve the model's prediction accuracy and stability, providing stronger support for widespread application.

Funding

This work was supported by Key Laboratory of Building Structures in Anhui Universities (Anhui Xinhua University) 2023 school-level scientific research project: "Application Research of BIM Technology in Cost Management of Engineering Construction Projects" (Project batch number: KLBSZD202301, Host: Wu Qian).

Conflict of interest statement

There is no conflict of interest in this study.

Ethical compliance statement

This study does not involve experiments on humans or animals and does not require ethical approval.

References

- [1] Li L. (2023). Dynamic cost estimation of reconstruction project based on particle swarm optimization algorithm. *Informatica*, 47(2), 173-182. <https://doi.org/10.31449/inf.v47i2.4026>
- [2] Maya, R., Hassan, B., & Hassan, A. (2023). Develop an artificial neural network (ANN) model to predict construction projects performance in Syria. *Journal of King Saud University-Engineering Sciences*, 35(6), 366-371. <https://doi.org/10.1016/j.jksues.2021.05.002>
- [3] Xu, X., & Zhang, Y. (2023). Regional steel price index forecasts with neural networks: evidence from east, south, North, central south, northeast, southwest, and northwest China. *The Journal of Supercomputing*, 79(12), 13601-13619. <https://doi.org/10.1007/s11227-023-05207-1>
- [4] GadelHak, Y., El-Azazy, M., Shibl, M. F., & Mahmoud, R. K. (2023). Cost estimation of synthesis and utilization of nano-adsorbents on the laboratory and industrial scales: A detailed review. *Science of The Total Environment*, 875, 162629. <https://doi.org/10.1016/j.scitotenv.2023.162629>
- [5] Abdel-Hamid, M., & Abdelhaleem, H. M. (2023). Project cost control using five dimensions building information modelling. *International Journal of Construction Management*, 23(3), 405-409. <https://doi.org/10.1080/15623599.2021.1880313>
- [6] Durstewitz, D., Koppe, G., & Thurm, M. I. (2023). Reconstructing computational system dynamics from neural data with recurrent neural networks. *Nature Reviews Neuroscience*, 24(11), 693-710. <https://doi.org/10.1038/s41583-023-00740-7>
- [7] Hai, T., & Zhou, J. (2023). Predicting the performance of thermal, electrical and overall efficiencies of a nanofluid-based photovoltaic/thermal system using Elman recurrent neural network methodology. *Engineering Analysis with Boundary Elements*, 150, 394-399. <https://doi.org/10.1016/j.enganabound.2023.02.013>
- [8] Das, S., Tariq, A., Santos, T., Kantareddy, S. S., & Banerjee, I. (2023). Recurrent neural networks (RNNs): architectures, training tricks, and introduction to influential research. *Machine Learning for Brain Disorders*, 117-138. https://doi.org/10.1007/978-1-0716-3195-9_4
- [9] Hananto, A. L., Fauzi, A., Suhara, A., Davison, I., Spraggon, M., Herawan, S. G., et al. (2023). Elman and cascade neural networks with conjugate gradient polak-ribière restarts to predict diesel engine performance and emissions fueled by butanol as sustainable biofuel. *Results in Engineering*, 19, 101334. <https://doi.org/10.1016/j.rineng.2023.101334>
- [10] Mahmoodzadeh, A., Mohammadi, M., Daraei, A., Farid Hama Ali, H., Ismail Abdullah, A., & Kameran Al-Salihi, N. (2021). Forecasting tunnel geology, construction time and costs using machine learning methods. *Neural Computing and Applications*, 33, 321-348. <https://doi.org/10.1007/s00521-020-05006-2>
- [11] Alshboul, O., Shehadeh, A., Almasabha, G., & Almuflih, A. S. (2022). Extreme gradient boosting-based machine learning approach for green building cost prediction. *Sustainability*, 14(11), 6651. <https://doi.org/10.3390/su14116651>
- [12] Pham, T. Q. D., Le-Hong, T., & Tran, X. V. (2023). Efficient estimation and optimization of building costs using machine learning. *International Journal of Construction Management*, 23(5), 909-921. <https://doi.org/10.1080/15623599.2021.1943630>
- [13] Goodarzizad, P., Mohammadi Golafshani, E., & Arashpour, M. (2023). Predicting the construction labour productivity using artificial neural network and grasshopper optimisation algorithm. *International Journal of Construction Management*, 23(5), 763-779. <https://doi.org/10.1080/15623599.2021.1927363>
- [14] Kim, S., Choi, C. Y., Shahandashti, M., & Ryu, K. R. (2022). Improving accuracy in predicting city-level construction cost indices by combining linear ARIMA and nonlinear ANNs. *Journal of Management in Engineering*, 38(2), 04021093. [https://doi.org/10.1061/\(ASCE\)ME.1943-5479.0001008](https://doi.org/10.1061/(ASCE)ME.1943-5479.0001008)
- [15] Ye, M., Wang, J., Si, X., Zhao, S., & Huang, Q. (2022). Analysis on dynamic evolution of the cost risk of prefabricated building based on DBN. *Sustainability*, 14(3), 1864. <https://doi.org/10.3390/su14031864>
- [16] Su, D., Fan, M., & Sharma, A. (2022). Construction of lean control system of prefabricated mechanical building cost based on Hall multi-dimensional structure model. *Informatica*, 46(3). <https://doi.org/10.31449/inf.v46i3.3914>
- [17] Cao, P., & Lei, X. (2023). Evaluating Risk in Prefabricated Building Construction under EPC Contracting Using Structural Equation Modeling: A Case Study of Shaanxi Province, China. *Buildings*, 13(6), 1465. <https://doi.org/10.3390/buildings13061465>
- [18] Leu, S. S., Lu, C. Y., & Wu, P. L. (2023). Dynamic-Bayesian-network-based project cost overrun prediction model. *Sustainability*, 15(5), 4570. <https://doi.org/10.3390/su15054570>
- [19] Asiedu, R. O., & Adaku, E. (2020). Cost overruns of public sector construction projects: a developing country perspective. *International Journal of Managing Projects in Business*, 13(1), 66-84. <https://doi.org/10.1108/IJMPB-09-2018-0177>
- [20] Kumar, R. (2022). Memory recurrent Elman neural network-based identification of time-delayed nonlinear dynamical system. *IEEE Transactions on Systems, Man, and Cybernetics: Systems*, 53(2), 753-762. <https://doi.org/10.1109/TSMC.2022.3186610>
- [21] Miranda, M. H., Silva, F. L., Lourenço, M. A., Eckert, J. J., & Silva, L. C. (2023). Particle swarm optimization of Elman neural network applied to

- battery state of charge and state of health estimation. *Energy*, 285, 129503. <https://doi.org/10.1016/j.energy.2023.129503>
- [22] Chandar, S. K. (2021). Grey Wolf optimization-Elman neural network model for stock price prediction. *Soft Computing*, 25(1), 649-658. [10.1007/s00500-020-05174-2](https://doi.org/10.1007/s00500-020-05174-2)
- [23] Zhang, Y., Zhao, J., Wang, L., Wu, H., Zhou, R., & Yu, J. (2021). An improved OIF Elman neural network based on CSO algorithm and its applications. *Computer Communications*, 171, 148-156. <https://doi.org/10.1016/j.comcom.2021.01.035>
- [24] Sohail, A. (2023). Genetic algorithms in the fields of artificial intelligence and data sciences. *Annals of Data Science*, 10(4), 1007-1018. <https://doi.org/10.1007/s40745-021-00354-9>
- [25] Chotchantarakun, K. (2023). Optimizing Sequential Forward Selection on Classification using Genetic Algorithm. *Informatica*, 47(9). <https://doi.org/10.31449/inf.v46i9.4964>
- [26] Guo, W., Meng, Q., Wang, X., Zhang, Z., Yang, K., & Wang, C. (2022). Landslide displacement prediction based on variational mode decomposition and GA-Elman model. *Applied Sciences*, 13(1), 450. <https://doi.org/10.3390/app13010450>
- [27] Wang, C., Zhao, Y., Bai, L., Guo, W., & Meng, Q. (2021). Landslide displacement prediction method based on GA-Elman model. *Applied sciences*, 11(22), 11030. <https://doi.org/10.3390/app112211030>